tRNA Discrimination at the Binding Step by a Class II Aminoacyl-tRNA Synthetase†

Michael L. Bovee, Wen Yan,‡ Brian S. Sproat,§ and Christopher S. Francklyn*

Department of Biochemistry, University of Vermont College of Medicine, Burlington, Vermont 05405

Received May 21, 1999; Revised Manuscript Received August 16, 1999

ABSTRACT: Aminoacyl-tRNA synthetases preserve the fidelity of decoding genetic information by accurately joining amino acids to their cognate transfer RNAs. Here, tRNA discrimination at the level of binding by *Escherichia coli* histidyl-tRNA synthetase is addressed by filter binding, analytical ultracentrifugation, and iodine footprinting experiments. Competitive filter binding assays show that the presence of an adenylate analogue 5′-*O*-[N-(L-histidyl)sulfamoyl]adenosine, HSA, decreased the apparent dissociation constant (K_D) for cognate $tRNA^{His}$ by more than 3-fold (from 3.87 to 1.17 μM), and doubled the apparent K_D for noncognate $tRNA^{Phe}$ (from 7.3 to 14.5 μM). By contrast, no binding discrimination against mutant U73 $tRNA^{His}$ was observed, even in the presence of HSA. Additional filter binding studies showed tighter binding of both cognate and noncognate tRNAs by G405D mutant HisRS [Yan, W., Augustine, J., and Francklyn, C. (1996) *Biochemistry 35*, 6559], which possesses a single amino acid change in the C-terminal anticodon binding domain. Discrimination against noncognate tRNA was also observed in sedimentation velocity experiments, which showed that a stable complex was formed with the cognate $tRNA^{His}$ but not with noncognate $tRNA^{Phe}$. Footprinting experiments on wild-type versus G405D HisRS revealed characteristic alterations in the pattern of protection and enhancement of iodine cleavage at phosphates 5′ to tRNA nucleotides in the anticodon and hinge regions. Together, these results suggest that the anticodon and core regions play major roles in the initial binding discrimination between cognate and noncognate tRNAs, whereas acceptor stem nucleotides, particularly at position 73, influence the reaction at steps after binding of tRNA.

The accuracy of protein synthesis in vivo relies on the ability of aminoacyl-tRNA synthetases (aaRSs)[1] to recognize and aminoacylate their cognate tRNAs in a highly specific two step reaction. In the first step, the aminoacyl adenylate is formed by condensation of amino acid with ATP. Subsequently, the amino acid is transferred to the 3′ end of the cognate tRNA (e.g., refer *2*). As a group, aaRS are surprisingly diverse in sequence and structure, yet they can be separated into two fundamentally distinct classes, each with a characteristic catalytic fold, consensus sequence motifs, and regiochemistry (*3*−*5*). Adenylation can occur in the absence of tRNA for the majority of the enzymes. In the cases of GlnRS[1] GluRS, and ArgRS, amino acid activation is dependent on prior tRNA binding. Thus, the influence of the first reaction on tRNA selection is not well understood, and is being evaluated in a number of systems (reviewed in refer *6*).

The molecular basis of amino acid and tRNA substrate specificity has been typically addressed for the aaRS in the context of the kinetics of the aminoacylation reaction. In general, nucleotide determinants that most strongly influence recognition are localized to the anticodon and the acceptor stem, but nucleotides in the tertiary core and other parts of the tRNA have also been observed to make significant contributions, as reviewed in (*7*−*9*). A recurring observation, emerging from these steady-state kinetic studies, is that alterations of recognition determinants typically, but not exclusively, exert a proportionately greater effect on k_{cat} than on K_m. This is in accord with the general picture that emerges from early work, namely that aaRSs exhibit less tRNA selectivity at the level of binding than at the level of catalysis (*10*, *11*).

These steady-state kinetics studies leave a number of key mechanistic questions unresolved, including the relative roles of individual steps, the relationship between Michaelis and affinity constants, and the identity of the rate determining step. Moreover, the relatively simplistic view of the kinetic basis for tRNA selection specificity has come under challenge by a growing body of high-resolution crystallographic data on the complexes of aaRS with their cognate tRNAs. For GlnRS and AspRS, the detailed physical descriptions

† This investigation was supported by USPHS NIH Grant GM54899 (C. S. F.) and Individual NRSA 1 F32 GM19739-01 (M. L. B.).

* To whom correspondence should be addressed. Professor Christopher S. Francklyn, Department of Biochemistry, University of Vermont College of Medicine, Health Sciences Complex C-444, Burlington, VT, 05405. Telephone: 802-656-8450. Fax: 802-862-8229. E-mail: franck@emba.uvm.edu.

‡ Present address: Department of Molecular Genetics, University of Texas, M.D. Anderson Cancer Center, 1515 Holcombe Blvd., Houston, TX 77030.

§ Present address: Innovir GMbH, Olenhuser Landstr. 20A, D-37124, Rosdorf, Germany.

[1] Abbreviations: aaRS, aminoacyl-tRNA synthetase; EDTA, (ethylenedinitrilo) tetraacetic acid; HSA, 5′-*O*-[N-(L-histidyl)sulfamoyl]-adenosine; NTP, nucleoside triphosphate; s*, apparent sedimentation constant. Following the standard convention, aminoacyl-tRNA synthetases are referred to by the three-letter code for their amino acid substrate, followed by the suffix RS.

10.1021/bi991182g CCC: $18.00
Published on Web 09/25/1999

of atomic contacts between the enzymes and their cognate tRNAs (*12*−*17*) are in good agreement with the biochemical and genetic data used to define recognition and identity determinants (*9*). However, in the complexes of the prolyl- (*18*), seryl- (*19*), and lysyl- (*19*, *20*) tRNA synthetases with their cognate tRNAs, large portions of the tRNA are missing in the electron density maps, implying static or conformational disorder in the crystals. The latter studies suggest the existence of binding states distinct from those of the yeast AspRS and GlnRS complexes, which could represent either an initial specific complex or a nonspecific complex. Significantly, the presence of a bound adenylate analogue in the SerRS−tRNA^{Ser} complex appears to order the 3′ end of the tRNA (*19*). This effect is mediated at least in part by a conformational change in the motif 2 loop, a class II-conserved structural feature within the catalytic site. The presence of the adenylate may, therefore, influence the recognition of the tRNA, a suggestion raised previously in the case of GlnRS and other systems (*21*, *22*). The consequences of bound adenylate may involve conformational rearrangements in both enzyme and tRNA that occur after binding but prior to aminoacylation. These observations raise the question of how much specificity is exerted at the binding step, and whether the effect of the adenylate product on initial recognition and specificity-determining events is general among aaRSs.

The HisRS system in *Escherichia coli* is particularly suitable to address these issues, since the enzyme's three-dimensional structure has been solved (*23*), a plausible mechanism for adenylation has been proposed (*50*), and the recognition determinants for tRNA^{His} have been shown to be dominated by the unique G^{-}1•C73 base pair located at the end of the acceptor stem (*24*, *25*). In particular, the C73 discriminator base has a profound effect in dictating the identity of histidine tRNA in vivo (*25*). Additional genetic and biochemical data indicate that relatively modest changes in binding interactions apparently can lead to significant changes in tRNA identity, underscoring the importance of steps prior to aminoacylation (*26*). The current investigation was undertaken to examine the role of tRNA binding in the specificity of tRNA selection. In particular, we sought to examine the influence of the adenylate product on the initial tRNA binding interaction, the extent of discrimination of the G1−C73 principal determinant at the level of binding, and the role of anticodon recognition in these processes.

MATERIALS AND METHODS

Chemicals and Reagents. The histidyl-adenylate analogue, 5′-*O*-[N-(L-histidyl)sulfamoyl]adenosine (HSA), was synthesized by Dr. Brian Sproat, Innovir. Restriction endonucleases *Eco*T22 I and *Bst*N I used in the preparation of tRNA transcripts were purchased from Amersham and New England Biolabs, respectively. NTPs were supplied by Pharmacia. Nonspecific yeast RNA included in filter binding reactions was purchased from Boehringer Mannheim.

Protein Expression and Purification. The wild-type (wt) *E. coli* HisRS enzyme was purified as described previously (*27*). Purification of the G405D mutant HisRS, which contains an N-terminal His_6 affinity tag, is described in detail in (*26*). In that study, it was shown that the presence of the affinity tag does not appreciably alter the kinetics of the aminoacylation reaction. The concentration of HisRS in all preparations was determined by absorbance at 280 nM, using an extinction coefficient of 127 097 M^{-1} cm^{-1}. These concentrations are invariably in good agreement with those determined by active-site titrations. Enzymes were stored at −20 °C in buffer D (50 mM Tris-HCl, pH 7.5, 100 mM NaCl, 10 mM $MgCl_2$, 1 mM β-ME, and 0.1 mM EDTA), containing 50% (v/v) glycerol and diluted directly for use in most experiments. Prior to analytical ultracentrifugation experiments, the enzyme was dialyzed at 4 °C against a 1000-fold excess of glycerol-free buffer D.

tRNA Transcription and Purification. Transcripts based on the sequence of tRNA^{His} from *E. coli* were prepared essentially as described previously in (*26*, *28*). The plasmid encoding the *Saccharomyces cerevisiae* tRNA^{Phe} gene was graciously provided by Dr. Olke C. Uhlenbeck, University of Colorado. Purified *E. coli* tRNA^{Thr} was a generous gift from Anne-Catherine Dock-Bregeon, IGBMC, Illkirch, France. Briefly, 4 mL transcription reactions were prepared in 40 mM Tris, pH 8.1, and contained 125 μg/mL template DNA, 4 mM each NTP, 20 mM GMP, 100 μg/mL T7 RNA polymerase. Reactions were quenched with 50 mM EDTA after 5 h incubation at 37 °C, and nucleic acid was extracted with phenol/chloroform (1:1) and precipitated with ethanol. The sample was resuspended in 6 M urea, and tRNA from up to four reactions was separated by continuous electrophoretic elution from an 11% polyacrylamide/7 M urea gel using a commercially available apparatus (Prep Cell, Bio-Rad). Fractions containing full-length tRNA were pooled, concentrated by centrifugal ultrafiltration (Centriplus-10, Amicon), and quantified by absorbance at 260 nm (1 AU = 33 μg/mL) prior to use in experimental assays.

Filter Binding Assays. HisRS−^{32}P-tRNA complex formation was monitored using the classical filter binding method of Yarus and Berg (*29*), with modifications described by Wong and Lohman (*30*) and Silvian (*22*). In this revised method, reactions were filtered through a three-layer membrane sandwich. The top layer (HT-Tuffryn, 0.45 μm porosity, Gelman Sciences) consists of polysulfone, which retains large nonspecific aggregates of protein and RNA. The middle layer is nitrocellulose (BA-85, 0.45 μm, Schleicher and Schuell) for retention of the specific protein/RNA complex. The bottom layer is positively charged nylon (Hybond-N+, Amersham), for quantitative capture of unbound tRNA. It is important to note that the useful pH range for this method is restricted. In the case of several aaRS−tRNA complexes, retention on nitrocellulose undergoes a marked decrease in efficiency above pH 5.5 (*29*). Amido black staining of the membranes showed that, within the limits of visual detection, all protein was captured quantitatively on the nitrocellulose layer. Membranes were equilibrated in buffer F (50 mM potassium phosphate, pH 5.7, 10 mM $MgCl_2$, 1 mM β-ME, 0.1 mM EDTA, 50 mM NaCl) for at least 10 min before assembly of the 96-well filtration apparatus (Minifold I, Schleicher and Schuell). All reactions were prepared in wash buffer plus 50 μg/mL BSA, 5 μg/mL yeast RNA (Boehringer Mannheim), and 10 nM tRNA that was labeled by incorporation of [α-^{32}P]UTP using standard methods (*31*). Depending on the experiment, reactions additionally contained 0−4 μM HisRS, and 0−3 μM competitor tRNA, as indicated in the figures. After incubation at ambient temperature (23 °C) for 5 min,

reactions (0.1 mL) were filtered through the membrane sandwich, followed by 0.6 mL of buffer F. The filters were removed from the apparatus and air-dried prior to quantitation. Use of this method allowed both bound and free populations of [α-^{32}P]UTP body-labeled tRNA molecules to be quantified by autoradiographic image analysis using a GS-525 phosphorimager and the Multi-Analyst software package version 1.0.2 (Bio-Rad).

The data from direct binding experiments were plotted as fractional saturation versus increasing enzyme concentration. A fractional saturation of unity was defined as the quantity of specific complex retained on the nitrocellulose at the highest enzyme concentration tested, relative to background in the absence of HisRS enzyme. Apparent K_D values were estimated by fitting the data to the simple binding isotherm:

$$\theta = \frac{[\text{enzyme}]}{[\text{enzyme}] + K_D} \quad (1)$$

where θ is the fractional saturation of enzyme/tRNA complex retained on the nitrocellulose, and K_D is the apparent dissociation constant for tRNA. Under the experimental conditions used, direct tRNA binding was saturable only for the cognate transcript. For competitive binding experiments, the enzyme and ^{32}P-tRNA concentrations were fixed at 500 and 10 nM, respectively, and fractional saturation was defined as unity in the absence of unlabeled competitor tRNA for each data set. Data were fit to the Lin and Riggs equation (*32*) using Deltagraph version 4.0.5 for the Macintosh computer. As described by Weeks and Crothers (*33*), solving this quadratic expression for θ gives the following physically relevant root:

$$\theta = \frac{1}{2T_t}(K_T + (K_T/K_C)C_t + T_t - \sqrt{[K_T + (K_T/K_C)C_t + T_t]^2 - 4T_tP_t}) \quad (2)$$

The parameters P_t, T_t C_t, K_T, and K_C represent total concentrations of enzyme, labeled cognate tRNA probe, competitor tRNA, and dissociation constants for the labeled cognate and unlabeled competitor tRNAs, respectively. The competition curve, $\theta = f(C_t)$, was fit for the best value of K_C using nonlinear regression analysis. The relative dissociation constant K_{rel} was defined as the ratio of noncognate to cognate values of K_C.

Analytical Ultracentrifugation. Sedimentation velocity experiments were conducted at 50 000 rpm and 20 °C in an Optima XL-I analytical ultracentrifuge (Beckman) equipped with an An50Ti rotor, and sample cells containing 12 mm double sector charcoal-filled Epon centerpieces and sapphire windows. Initial loading concentrations of HisRS or tRNA were 0.2 mg/mL (2.5 μM) and 0.125 mg/mL (5 μM), respectively, in a volume of 0.4 mL. Reactions were prepared in either buffer F (pH 5.7) or buffer D (pH 7.4). Sedimentation was monitored by absorbance at 280 nm. All sedimentation coefficients are reported in units of Svedbergs. Apparent sedimentation constants and g(s*) values were determined from raw data scans using the time derivative of the concentration profile, as described by Stafford (*34*). Some of the data were fit to Gaussian functions using Igor Pro, version 3.1 for Macintosh (WaveMetrics, Inc.). Molecular mass of the complex was estimated from the apparent sedimentation constant, s*, using the following equation, which is a combination of the Stokes and Svedberg equations:

$$s = 0.01\frac{(M^{2/3})(1 - \bar{\nu}\rho)}{\bar{\nu}^{1/3}} \quad (3)$$

where M is mass of the solute in Daltons, $\bar{\nu}$ is the partial specific volume of the solute, and ρ is the density of the solvent. The program SEDNTERP (*35*) was used to calculate the mass of HisRS (96 577 Da) as well as its $\bar{\nu}$ (0.734) based on amino acid sequence. For the $\bar{\nu}$ of tRNA little or no experimental data is available, so calculations were made using a range of $\bar{\nu} = 0.50-0.55$, based on comparison to values for DNA from an older report (*36*). Resulting weighted $\bar{\nu}$s for enzyme/tRNA complexes were 0.682 for one HisRS homodimer and one tRNA, or 0.650 for HisRS with two tRNAs bound. The densities for the two buffers were estimated using SEDNTERP; Buffer F has a calculated density of 1.00816 g/mL, while that of buffer D is 1.00420 g/mL.

Iodine (I_2) *Footprinting*. The templates for in vitro transcription of tRNA^{His} were derived from pWY40 (*26*). Each of the four phosphorothioate analogues (NTPαS) was separately incorporated into tRNAs at 5% (0.2 mM) of the concentration of the corresponding NTP to ensure an average of one phosphorothioate per tRNA molecule. The tRNA transcript yield was quantified by absorbance at 260 nm followed by purification on 12% polyacrylamide gels as described in (*26*). Transcripts were visualized by UV shadowing and eluted from gel slices by diffusion overnight at 4 °C into 0.5 M NH_4OAc, 1 mM EDTA, and 0.1% SDS. After ethanol precipitation, tRNA transcripts were dissolved in 10 mM sodium cacodylate buffer (pH 6.0), heated to 60 °C, and cooled slowly to 25 °C to fold the tRNA. 300 pmol of each transcript was incubated with 30 units of Calf Intestinal Alkaline Phosphatase (CIP) at 37 °C for 1 h to remove 5′-phosphates. After ethanol precipitation, the phosphatase-treated tRNAs were 5′-end labeled with [γ-^{32}P]ATP by T4 polynucleotide kinase (*37*). The labeled tRNAs were then separated on denaturing 12% polyacrylamide gels. Gel slices containing full-length transcripts were excised using the autoradiogram as a guide, soaked overnight at 4 °C in elution buffer, and the tRNA was recovered by ethanol precipitation. For RNA footprinting, 5×10^5 Cerenkov counts (approximately 0.2 μCi) of each of labeled tRNA (1−5 μL) was mixed with 2.5 μM unlabeled tRNA in 40 μL total volume, heated to 80 °C for 2 min, 60 °C for 3 min, and immediately mixed with 30 μL of footprinting buffer (33 mM NaCl, 33 mM $MgCl_2$, 33 mM Hepes, pH 7.5). Aliquots of 14 μL were dispensed into tubes, mixed with 4 μL of 4 μM HisRS (wt or G405D), and incubated at room temperature for 2 min before 2 μL of concentrated iodine were added to start the cleavage reaction. Control experiments contained water in the place of enzyme. After 2 min at ambient temperature, the reaction was stopped by addition of 80 μL of 0.4 M NaOAc at 4 °C. Following phenol/chloroform extraction, ethanol was added to precipitate RNA in the presence of glycogen. Reaction products were separated on denaturing 10% polyacrylamide sequencing gels and visualized by autoradiography. Exposed films

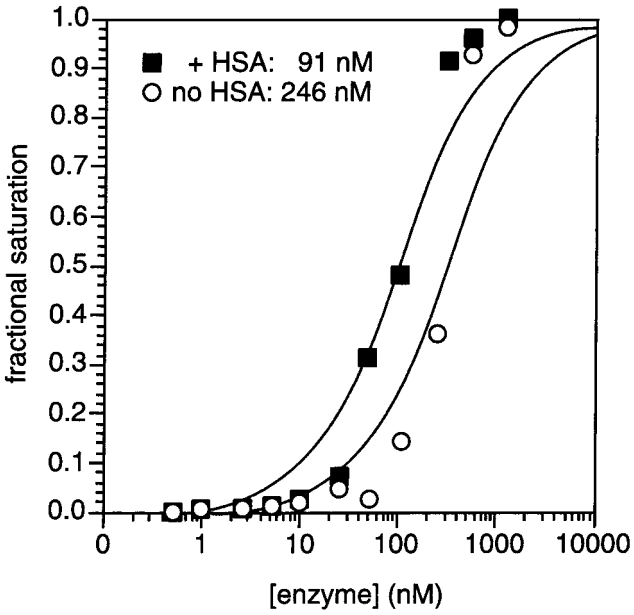

FIGURE 1: Direct nitrocellulose filter binding assay of the HisRS−tRNA^{His} cognate complex. The fractional saturation of tRNA binding by the specific complex was fit to a simple binding isotherm as described in Materials and Methods. Enzyme (0−4 μM) with or without the prebound adenylate analogue, HSA, was incubated with 10 nM ^{32}P-UTP body-labeled cognate tRNA and filtered as detailed in the Methods. Apparent dissociation constants for tRNA binding in the presence or absence of HSA are indicated.

were scanned and relative band intensities were quantified by densitometry using Multi-Analyst (Bio-Rad).

RESULTS

A Non-Hydrolyzable Histidyl-Adenylate Analogue Increases Cognate tRNA Binding Affinity. In previous work, specific information about the binding of tRNA^{His} by HisRS was obtained by determination of steady-state kinetic parameters for aminoacylation (*24*, *26*, *38*). Although some information about binding is provided by the Michaelis constant, direct determination of the dissociation constant provides a quantitative measure of the relationship between K_m and K_D. To examine binding affinities directly, the classical filter binding procedure of Yarus and Berg (*29*) was used, with modifications developed by Wong and Lohman (*30*) and Silvian (*22*). As described in Materials and Methods, the technique was further adapted for studies on the histidine system through empirical optimization of the binding reaction pH. The fractional retention efficiency of the complex on the nitrocellulose reached 80% of the theoretical maximum as determined by the method of Draper et al. (*39*) (data not shown). Apparent dissociation constants (K_D) were measured by titrating HisRS from 0 to 4 μM against 10 nM tRNA, well below the predicted dissociation constant based on other aaRS systems (*22*, *40*). The data were then fit to a simple binding isotherm, allowing a dissociation constant of 246 nM to be determined for the cognate interaction. Binding of the histidyl-adenylate analogue, 5′-*O*-[N-(L-histidyl)sulfamoyl]adenosine (HSA), prior to addition of tRNA decreased the apparent K_D for tRNA approximately 2.5-fold, to 91 nM (Figure 1). Estimates of K_D from direct binding experiments using tRNA^{Phe} were not possible due to an inability to reach saturation of the enzyme with the labeled noncognate tRNA. This problem was overcome by measuring K_D for both cognate and noncognate tRNAs under competitive binding conditions as described below.

As an alternative method for measuring dissociation constants of the HisRS/tRNA complex, competitive filter binding assays were also carried out. Since competition for tRNA binding in vivo is a critical parameter for substrate selection, these assays can be expected to better model the interaction than the direct binding assays. Complexes formed between HisRS and labeled cognate tRNA were challenged with varying concentrations of unlabeled competitor tRNAs and filtered using the three membrane sandwich method described above. The data were fit to a form of the Lin and Riggs equation (*32*) used by Weeks and Crothers (*33*), to determine dissociation constants for the competitor tRNAs. As shown in Figure 2 and Table 1, the presence of HSA increased the affinity of HisRS for wt tRNA^{His} 4-fold (3.87 $\pm$ 0.54 μM in the absence of analogue versus 1.17 $\pm$ 0.15 in its presence), and had a 2-fold effect on the affinity for tRNA^{Phe} (7.3 $\pm$ 0.1 μM in the absence of analogue versus 14.5 $\pm$ 5.5 μM in its presence). Some global variability in K_D was observed among independent experiments, particularly for the noncognate tRNA. Within each experiment, the ratio of K_D values for noncognate to cognate tRNAs was more consistent. For this reason, the K_{rel} parameter (defined here as the ratio of dissociation constants for the noncognate versus cognate tRNA) is useful. K_{rel} values listed in Table 1 indicate that the adenylate analogue raises the discrimination against noncognate tRNA from less than 2-fold in its absence to 10-fold in its presence. A similar set of assays was carried out using U73 tRNA^{His} transcripts, and the affinities for this mutant tRNA in the presence or absence of HSA analogue were not significantly altered from the values determined with the wt (C73) tRNA^{His} (Table 1). Thus, discrimination against U73 at the binding step was not detectable in these assays, which is consistent with the relatively minor effect on K_m reported in (*24*, *26*). In the case of GlnRS, acceptor stem contacts critical for tRNA recognition were also found to contribute only slightly to the binding energy of the complex (*21*). An additional competitive binding experiment was conducted using tRNA^{Thr} as a competitor. This tRNA was chosen because it contains all in vivo modifications, and the corresponding ThrRS is also a class IIa enzyme. Results indicated that modified tRNA^{Thr} was a poor competitor for binding to HisRS in the presence of tRNA^{His} and its behavior in the presence and absence of HSA was equivalent to that of the tRNA^{Phe} transcripts (data not shown).

One inherent limitation of the filter binding assays is the inability to distinguish between nonproductive binding and binding that may be productive with respect to aminoacylation. Previously, Michaelis constants (K_m) for transcripts based on tRNA^{His} in the aminoacylation reaction were determined to be in the range of 0.5−1.5 μM (*26*, *38*). The agreement between K_m for aminoacylation and the dissociation constants measured here by direct and competitive methods suggests that the data reflect productive binding. To a first approximation, the value for K_D is similar to that for K_m, and the system appears to be in rapid equilibrium.

Dissociation Constants for a K_m Mutant of HisRS Reflect Alterations in tRNA Binding. In previous work, two *hisS* compensatory mutants (G405D HisRS and G96D/R104H HisRS) were generated from in vivo selections against U73 amber suppressors of tRNA^{His} (*26*). These HisRS mutants

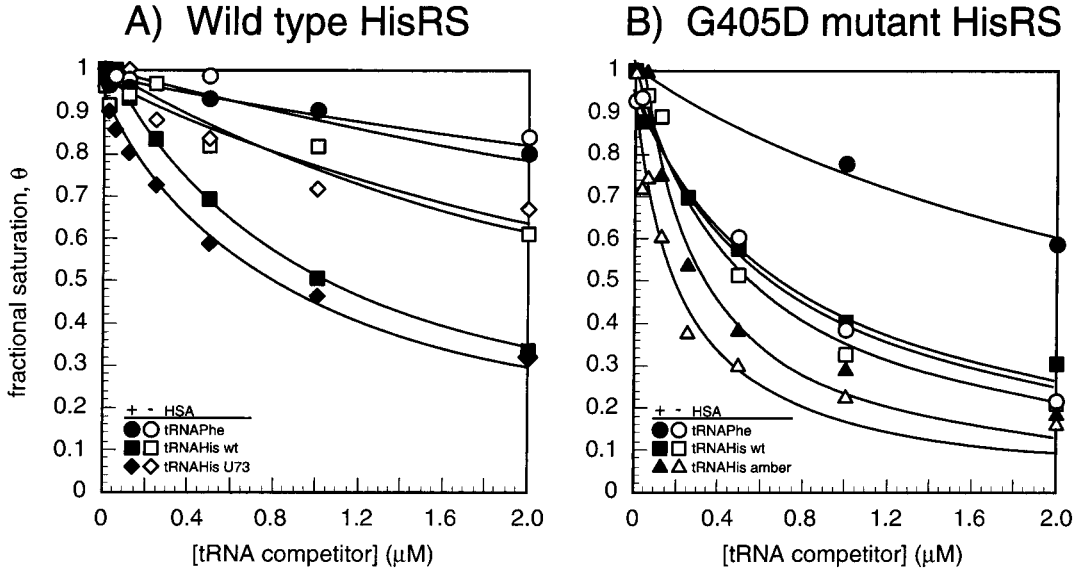

FIGURE 2: Competitive binding of the wt HisRS or G405D HisRS−^{32}P-tRNA^{His} complex by various unlabeled competitor tRNAs. Enzyme with (shaded symbols) or without (open symbols) prebound HSA was incubated with labeled cognate tRNA prior to the addition of competitor tRNAs as described in the methods. (A) Wt HisRS with various competitor tRNAs. (B) G405D mutant HisRS with competitor tRNAs. Competitor tRNAs are as indicated: cognate tRNA^{His} transcript (C73, squares); mutant tRNA^{His} substituted with uracil at the discriminator position 73 (U73, diamonds); amber suppressor (CUA) tRNA^{His} (Amber, triangles); and *S. cerevisiae* tRNA^{Phe} transcript (Phe, circles). Data were fit to a form of the Lin and Riggs equation as described in Materials and Methods.

Table 1: Apparent Dissociation Constants for tRNA from Competitive Filter Binding Experiments[a]

		tRNA				
HisRS	HSA[b]	His wt	His U73	His amber	Phe	K_{rel}[c]
wt	−	3.87 ± 0.54	3.24[d]	0.89	7.3 ± 0.1	1.89
wt	+	1.17 ± 0.15	0.91	0.29	14.5 ± 5.5	12.5
G405D	−	0.60 ± 0.07	ND	0.28 ± 0.07	0.76 ± 0.01	1.25
G405D	+	0.95 ± 0.23	ND	0.28 ± 0.04	2.33 ± 1.44	2.44

[a] Apparent dissociation constants (K_D) were measured at 23 °C and pH 5.7. K_D values and standard deviations were determined using at least two data sets and are reported in units of micromolar (μM). [b] Non-hydrolyzable histidyl-adenylate analogue. [c] K_{rel} is the ratio of K_D (Phe) to K_D (His wt). [d] Data without error values are from a single experiment. ND, not determined.

exhibited significant decreases in the apparent K_m for aminoacylation of tRNAs with the amber suppressor anticodon. In a docking model using HisRS coordinates (*23*) and those of tRNA^{Asp} from its complexed form with AspRS (*16*), the G405D substitution localized to the C-terminal domain of HisRS and was predicted to be in close proximity to the anticodon nucleotide G36 (*26*). In light of these findings, the effect of the G405D mutation was examined in the competitive filter binding assay for its ability to discriminate between tRNA^{His} and noncognate tRNA^{Phe}. Figure 2 shows that in contrast to the wt protein, the affinity of G405D HisRS for wt tRNA^{His} was slightly decreased in the presence of the analogue (K_D 0.60± 0.07 μM without analogue versus 0.95 ± 0.23 in its presence, Table 1). A smaller difference in binding discrimination against noncognate tRNA^{Phe} in comparison to the wt enzyme was also observed, (0.76 ± 0.01 without analogue versus 2.33 ± 1.44 in its presence) and suggests that the anticodon binding domain mutation is associated with a global reduction in binding discrimination. The G405D mutant was also tested with an amber suppressor variant of tRNA^{His}, as previous work had demonstrated a preferential decrease in K_m for this substrate. Consistent with these earlier observations, a slight increase in affinity was observed over the wt tRNA substrate. These data are consistent with the idea that the affinities measured by competitive filter binding are dominated by interactions between the anticodon arm of the tRNA and the anticodon binding domain of the synthetase. The molecular basis for the slight increase in affinity observed for G405D HisRS is currently under investigation, but may be related to an increase in the contribution of nonspecific binding. On the basis of experiments conducted previously on G405D HisRS (*26*), contacts with the cognate tRNA contributed by the anticodon binding domain appear to strongly influence the overall binding affinity and specificity of the complex in vivo.

Detection of the Cognate Complex by Analytical Ultracentrifugation. While there is ample precedent for the use of filter-binding assays to measure the affinities of aaRS−tRNA complexes, the technical requirement for a pH below physiologic conditions suggests that caution must be exercised in their interpretation. As an alternative procedure for addressing the specificity of aaRS-tRNA interactions unhampered by pH restrictions or problems arising from immobilization on membrane filters, analytical ultracentrifugation (AUC) allows direct detection of free and complexed components and imposes no requirement for radioactive labels. On the basis of the earlier work of other researchers (*40, 41*) and the fact that K_D and K_m are comparable in magnitude, it is reasonable to assume that the aaRS−tRNA interaction is in fast exchange in relation to the time scale of sedimentation. Equilibrium is, therefore, established at all positions in the sample cell (*42*). For these experiments, the distribution of a species and its respective apparent sedimentation coefficient, s*, was quantified using the time derivative of the concentration profile (*34*), as opposed to the radial derivative. This method is independent of time-invariant contributions to the optical baseline, and thus results in a higher signal-to-noise ratio. In practice, this permitted

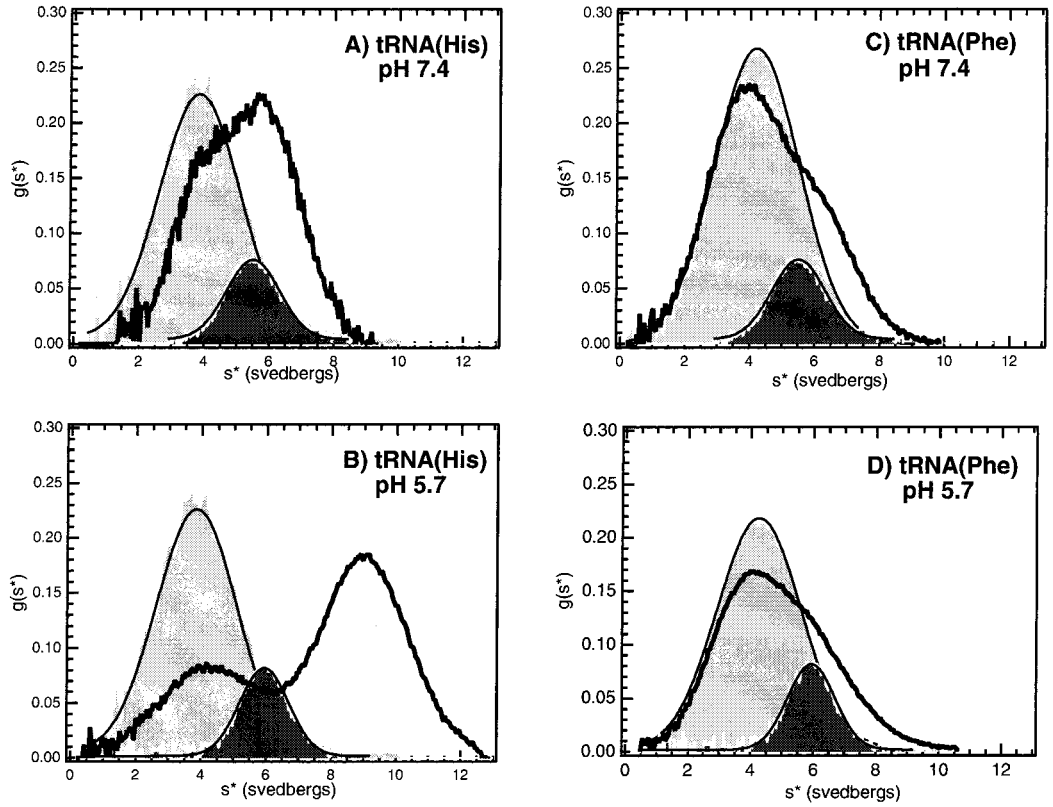

FIGURE 3: Sedimentation velocity analysis of the complex between wt HisRS and $tRNA^{His}$ or $tRNA^{Phe}$. (A) Complex formation with $tRNA^{His}$ at pH 7.4 or (B) pH 5.7. (C) Cosedimentation of HisRS and $tRNA^{Phe}$ at pH 7.4 or (D) pH 5.7. The *y*-axis, g(s), is proportional to concentration as described by Stafford (*34*), and the *x*-axis shows the distribution of sedimenting species from smallest to largest (left to right). Control experiments show the corresponding g(s) sedimentation profile of the free enzyme (dark shaded peaks) and free tRNAs (light shaded peaks).

data collection at the relatively low initial loading concentrations of 2.5 μM enzyme and 5 μM tRNA.

The sedimentation properties of free $tRNA^{His}$, HisRS-adenylate, and HisRS-adenylate + tRNA in buffer D (pH 7.4) or buffer F (pH 5.7) were independently measured using an absorbance optical system. Free $tRNA^{His}$ or $tRNA^{Phe}$ reproducibly sedimented as nonassociating species best described by a single Gaussian function with a maximum at $s^* = 3.8$ or 4.2, respectively, and both tRNAs were unaffected by pH (Figure 3, light gray peaks). These values are in excellent agreement with those reported previously for tRNA (*42*). HisRS-adenylate also sedimented as a nonassociating species with some pH-dependent variance in the sedimentation constant; $s^* = 5.4$ in buffer D, versus 5.9 in buffer F (Figure 3, dark gray peaks). Control experiments lacking the HSA analogue were in close agreement with these findings, suggesting that the presence of the analogue does not significantly alter the sedimentation properties of HisRS.

The specificity of complex formation was addressed by sedimentation velocity experiments on enzyme and tRNA together under both pH conditions. Analysis of the distribution of sedimenting species for HisRS/histidyl-adenylate and $tRNA^{His}$ in buffer F resulted in two peaks, each of which was described by a Gaussian function. The left peak (slowest sedimentation) had a maximum at $s^* = 3.8$ and the right peak (fastest sedimentation) had a maximum at $s^* = 9.0$. The s* value for the first peak is in excellent agreement with that of the free tRNA (*42*) and Figure 3, light gray peaks), while the second peak sediments faster than either the free tRNA or free enzyme, and suggests the formation of a stable enzyme−tRNA complex. After eq 3 was applied as described in the Materials and Methods, the apparent *S* value of the complex was estimated to be 8.5 in the case of a 1:1 complex or 10.8 in the case of 1:2 complex. Because s* also depends on shape, these values are estimates since $\bar{\nu}$ for tRNA has not been explicitly determined. On the basis of the criteria assigned above, these data support the detection of a 1:1 complex at pH 5.7, even when a range of values from 0.5 to 0.55 are substituted for the partial specific volume of the tRNA (see Methods). At pH 7.4, this complex is not detected, although a shift in the distribution of the tRNA occurs in a manner that resembles a reacting sedimentation boundary, in which the free components and the complex do not resolve as independent species. Under these conditions, the mass of the complex and binding stoichiometry cannot be estimated by sedimentation velocity. However, in light of the relatively modest tRNA-binding affinities determined above and by others, these data likely reflect a rapid equilibrium between free and bound tRNA at the higher pH and higher salt concentration. At the lower pH, dissociation of the tRNA is presumed to be much slower. More rigorous determination of the mass of the complex is being investigated by sedimentation equilibrium analysis, and those results will be reported separately. When $tRNA^{Phe}$ was used in place of $tRNA^{His}$, the g(s) profile in either buffer was only slightly shifted relative to the sum of the Gaussian functions for the free components, indicating neither the formation of a stable complex nor a reacting boundary. Our results from AUC analysis are consistent with those from filter binding and show that the HisRS−$tRNA^{His}$ complex is stable and exhibits

strong specificity for cognate tRNA even at pH 5.7. This is in sharp contrast to noncognate $tRNA^{Phe}$, which did not appreciably interact with HisRS in solution. We assume that under these conditions equilibrium was reliably established, suggesting that tRNA discrimination at the binding step is sufficient for the rejection of noncognate tRNA.

Iodine Footprinting of wt HisRS on Phosphorothioate-Substituted $tRNA^{His}$ Shows a Recognition Pattern Characteristic of a Class II aaRS. We have argued above that the close correspondence between K_Ds determined by filter binding and the K_ms determined from steady-state kinetics suggest that the binding observed in solution represents a specific and productive complex as opposed to a nonproductive complex. To further investigate this issue, footprinting experiments were performed using the small chemical probe iodine to cleave the tRNA backbone at the substituted phosphorothioate groups. The interpretation of these results is facilitated by crystallographic data available for complexes of class II aaRS with their cognate tRNAs (*16*, *17*, *19*, *20*, *43*). As shown by the excellent agreement between protected phosphates and crystallographic contacts observed in the seryl- and aspartyl- systems, a subset of these protected phosphates likely constitutes those in direct contact with the enzyme (*16*, *19*, *44*, *45*). By contrast, positions where cleavage is enhanced may be the result of indirect effects mediated by the bound protein, signaling a structural change in the tRNA. By testing a range of iodine concentrations (100−500 μM), we observed that higher iodine concentrations maximized the distinction between protected and nonprotected sites, so 400 μM iodine was used for most of the experiments described here. Analysis of control experiments with the class IIa ProRS did not reveal evidence of protection, a further indication that the contacts are specific for the HisRS−$tRNA^{His}$ complex (data not shown). Additional controls showed that the cleavages observed were dependent on the presence of iodine, and that the extent of protein-mediated cleavage in the absence of iodine was minimal (data not shown).

The data from footprinting experiments are shown in Figure 4 and are summarized on cloverleaf representations of tRNA in Figure 5. The presence of HisRS resulted in strong protection (40−70% decrease in band density) of a number of internucleotide phosphates located 5′ to their respective bases (Figure 5A, solid arrows) in the acceptor stem (G3), in the D-stem and -loop (G10·C25, C13, G15, G18, G26), the anticodon stem and loop (C27, U28, G29, G36, A37, U38) and the TΨC loop (U54 and U55). Weaker protection corresponding to a 20−40% decrease in band density (Figure 5A, open arrows) was observed at additional 5′-phosphates in the acceptor stem (U6), D-stem (G24), anticodon stem (G30, A31), variable loop (G46) and TΨC stem and loop (G52, G53, C56, G57). At the highest iodine concentrations, protection 5′ to U6, C13, and C25−C27 was significantly diminished, suggesting that these nucleotides may be only transiently in contact with HisRS. Owing to limits in resolution imposed by electrophoretic separation of the cleavage products, no conclusions can be drawn about positions outside the detected range of nucleotides 3−60.

These data indicate that HisRS protects significant portions of both the acceptor stem (e.g., near nucleotides 3, 5, and 6) and the anticodon arm (nucleotides 36 and 37), which is in good agreement with the effects that mutations in these

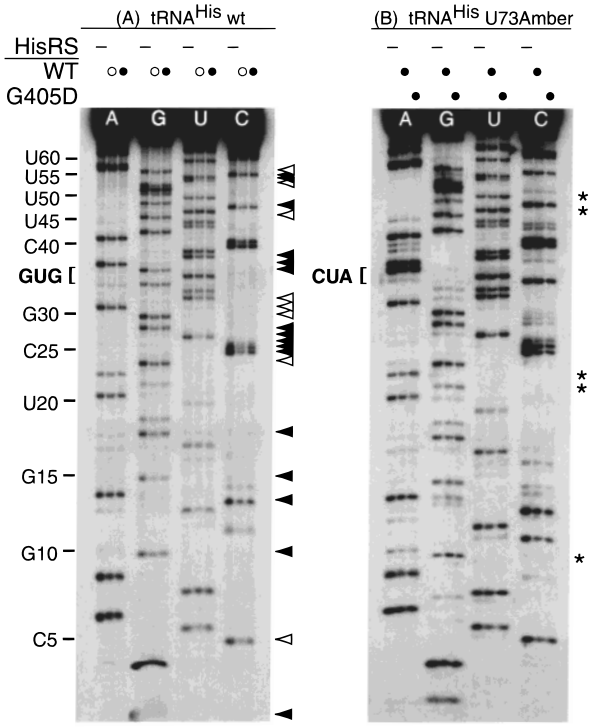

FIGURE 4: Iodine footprinting of wt and G405D HisRS complexed with phosphorothioate-substituted $tRNA^{His}$ transcripts. Footprinting reactions and acrylamide gel analysis methods are described in the Methods. (A) Footprinting protection pattern of the wt HisRS on wt $tRNA^{His}$ (C73, GUG) at 300 (open circles) and 400 μM iodine (closed circles). (B) Footprinting protection pattern of the wt and G405D mutant HisRS on U73 amber mutant tRNA (U73, CUA). Dashes above lanes, no enzyme. Circles above the lanes, presence of wt or mutant HisRS in the cleavage reactions as indicated on the left (400 μM iodine, closed circles). A histidyl-tRNA sequence ladder is shown in 5-nucleotide increments along the left side, with the anticodon triplet bracketed. Autoradiograms of dried gels were scanned and band intensities were quantified by densitometry. Strong protections, 40−70% decrease in band density (solid arrows); weak protections, 20−40% decrease in band density (open arrows). Enhanced cleavage in the presence of HisRS is denoted by an asterisk.

regions have on aminoacylation by the enzyme (*24*, *26*, *46*). Owing to the functional significance of acceptor stem and anticodon recognition in complexes between class II aaRS and their cognate tRNAs, these positions represent the most likely candidates for direct interactions with the enzyme (*16*, *19*, *47*). In addition, the protection of U28 and G29 may also reflect direct interactions, as these phosphates are candidates for cross-subunit interactions, as observed in ThrRS (*47*). Finally, a set of protections was observed that, as a consequence of their position on the D-stem loop face (e.g., 5′ to G15, G18, and G24) and TΨC loop (U55), are unlikely to be the result of direct protection by the enzyme. Protected phosphates inconsistent with those predicted from the X-ray structure of the complex were also reported in the case of AspRS (*45*). At least a subset of these are likely to reflect changes in the chemical reactivity of phosphorothioates that are mediated by local changes in tRNA structure occurring as a result of binding. Alternatively, it has been suggested that these indirect protections might represent weak interactions with other synthetase−tRNA complexes in solution (*45*).

Footprinting Experiments on Mutant tRNA Using wt or Mutant HisRS Reveal an Alternate Recognition Pattern. The

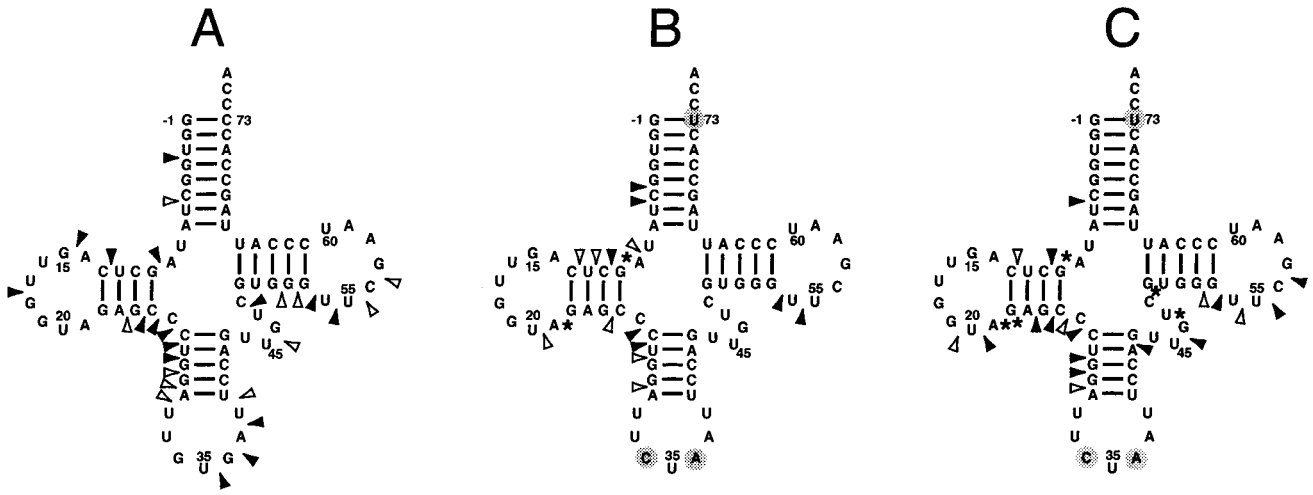

FIGURE 5: HisRS protection pattern on cloverleaf representations of $tRNA^{His}$ based on data from Figure 4. The sequences shown correspond to those of the unmodified transcripts on which the footprinting experiments were done. (A) wt HisRS on wt tRNA, (B) wt HisRS on U73 amber mutant tRNA, (C) G405D mutant HisRS on U73 amber mutant tRNA. Nucleotides mutated in U73 amber tRNA are shaded. Strong protections, 40−70% decrease in band density (solid arrows); weak protections, 20−40% decrease in band density (open arrows). Asterisks indicate enhanced cleavage in the presence of the respective enzymes.

cognate protection pattern described above suggests that recognition between the anticodon binding domain of HisRS and the anticodon of $tRNA^{His}$ occurs and is part of a productive interaction. The U73 amber tRNA was previously shown to be an extremely poor substrate for catalysis by both wt and G405D enzymes (*26*). As expected, footprinting analysis of wt HisRS on the mutant tRNA transcript showed substantial differences from the cognate protection pattern in three regions on the tRNA (compare Figure 5A with Figures 4B and 5B). These include loss of protection at phosphate groups in the anticodon loop (U32−U38), positions within the variable loop (G46, C48), and C56 and G57 within the TΨC loop. In addition, the presence of HisRS increased cleavage at phosphates 5′ to G10 (by 68%) and G22 (by 20%), which may indicate conformational changes in the tRNA core that are distal to interactions with the mutated residues (gray circles). These changes in the protection pattern underscore the clear correlation between diminished anticodon binding and reduced aminoacylation function for the wt enzyme. The fact that G405D mutant HisRS is capable of restoring histidine identity to U73 $tRNA^{His}$ amber in vivo indicates that the mutant tRNA is not misacylated by other aaRS and raises the possibility that at least some key features of the cognate complex have been restored. Surprisingly, the footprinting pattern of the G405D HisRS−U73 $tRNA^{His}$ amber complex (Figure 5C) differs from that of the homologous complex (Figure 5A) in at least two ways: First, protection has not been restored in the anticodon loop, nor at phosphate positions in the D-loop (5′ to G18) or the acceptor stem (5′ to G3). In addition, cleavage was enhanced at G10 and G22 as well as other sites on the tRNA, including the phosphates 5′ to A23 and especially U47 and U50. These sites are involved in canonical tertiary interactions in the tRNA core, reviewed in (*48*) and are responsible for the flexibility of the hinge. Conversely, several protections that are lost in the wt HisRS−U73 $tRNA^{His}$ amber complex (compare Figure 5B to 5A) are restored in the G405D HisRS−U73 $tRNA^{His}$ amber complex, including those 5′ to G24 in the D-stem, G46 in the variable loop, and C57 and G58 within the TΨC loop.

DISCUSSION

Despite rapid progress made in the last five years toward identifying tRNA identity elements, determining the precise enzyme functional groups responsible for imparting this specificity and characterizing the mechanistic basis of their mode of action has proven to be more elusive. A major principle established in early work is that aaRS restrict aminoacylation of noncognate tRNA to a greater extent at the level of V_{max} than at the level of K_m (*10*, *11*). This observation, along with the relatively modest affinities observed for tRNAs by synthetases, suggests that the amount of specificity that can be imposed at the binding step is considerably less than that of subsequent steps, especially catalysis and product release. These conclusions were based partly on observations that affinities for noncognate tRNAs (as approximated by K_m) were often within 1 order of magnitude of those of the cognate tRNA, and that the 3′ terminal trinucleotide apparently contributes little in the way of binding affinity (*49*, *50*). It is also evident from comparative studies of recognition in different tRNA systems (reviewed in refs *8*, *9*, and *46*) that important recognition determinants typically exhibit more pronounced effects on k_{cat} than on K_m. This implies that only minimal discrimination is exerted against noncognate tRNAs during initial binding events, and that major determinants in tRNAs have a proportionately greater role in steps following binding, including rearrangement, chemistry, and product release. Nevertheless, some specificity must be exerted at the binding step in order to prevent aaRS from engaging in nonproductive and nonspecific complexes that would lead to their sequestration in vivo.

The work presented here was undertaken to address the contribution of the tRNA binding step to tRNA selection in the *E. coli* HisRS system. The adenylation reaction step has been described in detail in (*23*, *51*). One objective of the present work was to evaluate the role of the adenylate product in tRNA binding. This question was addressed by use of competitive filter binding assays, which showed that the presence of histidyl adenylate raised the apparent discrimination between transcripts based on cognate $tRNA^{His}$ and

noncognate $tRNA^{Phe}$ from 2-fold to 10-fold (Table 1); a similar level of discrimination was also observed against fully modified $tRNA^{Thr}$. The presence of adenylate has an even greater effect on tRNA discrimination by GlnRS (*21*, *22*), and a role for the adenylate in providing increased ordering of the CCA end has been described for SerRS (*19*). One potential concern with the use of filter binding assays is that the pH must be below the physiological range. A pH of 5.7 was used in these studies. Others have reported that affinities are higher and interactions with tRNA are less specific than at pH 7.0. Dissociation constants for the interaction of PheRS with cognate $tRNA^{Phe}$ and an assortment of noncognate tRNA have been reported based on measurements using a variety of techniques, including fluorescence quenching (*52*), K_m measurements (*53*), filter binding (*54*), ultracentrifugation and fast kinetic techniques (*49*). While the strength of these noncognate interactions shows variation between systems, the apparent affinities for the HisRS−$tRNA^{His}$ interaction reported here are consistent with these earlier measurements, many of which were obtained at physiological pH (*49*, *52*). The dissociation constants measured in prior work range from 170 to 500 nM, and the 2.5-fold binding discrimination against non cognate tRNA observed by others (*55*) is comparable to the 2-fold discrimination reported here for HisRS in the absence of analogue. The agreement between our data and the measurements reported by others argues against the possibility of a major systematic error introduced as a result of the reliance on filter binding.

An additional concern for interpretation of these studies is the fact that the wild-type tRNAs were transcripts lacking the normal complement of modified bases. Although there is no evidence that any of the modifications of histidine tRNAs (e.g., the queuosine at position 34) are essential recognition components, there is prior work to suggest that transcripts require a higher magnesium concentration to reach the T_m of fully modified tRNAs, implying a reduction in tertiary structural stability (*56*). If, as we argue below, forming a productive complex with the enzyme requires obligatory conformational changes on the part of the tRNA, then this reduced structural stability would tend to reduce apparent discrimination. The fact that $tRNA^{Phe}$ transcripts and fully modified $tRNA^{Thr}$ behaved comparably indicates that this effect is likely to be minimal under our experimental conditions.

These conclusions about the rejection of noncognate tRNA at the level of binding were also supported by sedimentation velocity experiments, which showed that stable complexes with $tRNA^{Phe}$ do not form at either of the conditions tested. Notably, the interaction observed with the cognate tRNA at pH 7.4 in the presence of the HSA analogue was considerably weaker than that observed at pH 5.7. The sedimentation profile in analyses performed with the cognate complex at pH 7.4 resembles a reacting boundary and suggests that at this pH and salt concentration the enzyme and tRNA are in rapid equilibrium, implying a fast off rate for the tRNA. This suggestion of fast exchange is consistent with the relatively close correspondence between K_D and K_m, as was our inability to accurately measure off rates by filter binding (M. B. and C. S. F., unpublished observations). We can discount trivial explanations for the absence of a tight complex for HisRS at the higher pH, as a parallel analysis conducted with the related threonyl-tRNA synthetase resulted in stable complex formation in both of the buffers used here (M. B. and C. S. F., unpublished results). Thus, the binding reaction conditions used at the higher pH are not intrinsically unfavorable for the formation of stable complexes of aaRS with their tRNAs, as measured by the appearance of a faster sedimenting boundary. This would imply that there may be significant pH-dependent differences in cognate tRNA binding affinity for HisRS and ThrRS in vitro. A further interesting issue raised by our sedimentation analysis is the observed 1:1 stoichiometry of the complex at pH 5.7. Previous sedimentation studies by Krauss et al. (*49*) revealed a wide range of behavior among different aaRS, particularly with respect to the affinity and cooperativity of tRNA binding. Notably, PheRS was observed to bind two tRNAs with relatively high and equivalent affinities, whereas SerRS bound its two tRNAs with markedly unequal affinities. This latter behavior was similarly observed in the different crystal forms of the SerRS−$tRNA^{Ser}$ complex, which exhibited both 1:1 and 1:2 stoichiometries (*19*, *57*).

The binding studies performed here highlight the differential contributions of the acceptor arm and the anticodon arm to the specificity of the initial binding complex. Significantly, the binding affinity was equivalent for complexes that differed only by the presence of cytosine or uracil at position 73 in the tRNA, indicating that specificity for this critical nucleotide is not manifested in the binding reaction (Table 1). This observation is in excellent agreement with previous kinetic studies, and suggests that interactions with the 3′ proximal end of the acceptor stem provide little or no binding specificity. The behavior of HisRS in these binding experiments is analogous to that of AlaRS, which displayed comparable binding affinities and exhibited only slight (less than 3-fold) discrimination against noncognate base pairs at the 3:70 major determinant (*55*). The substitution of acceptor stem determinants in both the HisRS and AlaRS systems produces preferential decreases in k_{cat} (reviewed in ref *9*), and preliminary data in the HisRS system indicates that discrimination at base 73 is mediated by residues in the motif 2 loop (S. Hawko and C. Francklyn, manuscript in preparation). Thus, the current picture is that correct readout of acceptor stem nucleotides occurs after the initial binding event, and requires positioning interactions that are strongly influenced by contacts to the anticodon arm.[2]

By contrast, the anticodon−C-terminal domain interaction appears to play a far greater effect on the binding interaction between HisRS and its cognate tRNA than the acceptor stem. First, prior kinetic studies showed that substitutions of anticodon nucleotides preferentially increase K_m (*26*, *46*). In addition, previous kinetic analyses and the binding studies performed here showed that the C-terminal G405D substitution was associated with reduced binding discrimination between cognate and noncognate tRNA (Figure 2, Table 1). Moreover, iodine footprinting experiments showed that the anticodon is protected in the cognate complex, and that the substitution of nucleotides in the anticodon is associated with changes in protection that mirror the kinetic effects (Figure 5). The fact that these anticodon interactions apparently play

[2] Although neither AlaRS nor SerRS apparently make contact to the anticodon trinucleotide loop, footprinting experiments suggest that AlaRS contacts portions of the anticodon stem (*1*), and SerRS uses contacts to the tRNA variable arm to position the tRNA for transfer.

a much greater role in the initial tRNA binding event than their acceptor stem counterparts raises the possibility that anticodon binding precedes acceptor stem interactions, an idea implicit in those aaRS crystallographic complexes where density for the acceptor stem is absent (*18*−*20*).

These experiments provide additional support for an important model that is beginning to emerge from studies focused on the aaRS (reviewed in ref *6*). In this model a conformational change in the tRNA following the initial binding step is required to correctly position the acceptor end in the active site. The existence of conformational intermediates had been suggested earlier on the basis of fast kinetics studies (*58*). Increased attention is also being focused on this issue as a result of detailed structural comparisons among class II aaRS complexed with their cognate tRNAs. This is illustrated in the recent X-ray structure of the class IIa threonyl-tRNA synthetase with its cognate tRNA (*47*). A notable difference in this complex as compared to the related class IIa prolyl-tRNA synthetase with its cognate tRNA (*18*) is that in the ThrRS complex, base 38 has swiveled out of its stacked conformation in the anticodon loop to make a stacking interaction with Arg 583. The authors further suggest that this change is associated with a kink in the anticodon stem around the 30−40 base pair. Notably, base 38 in the prolyl complex maintains its stacking interactions with the anticodon stem, and the acceptor stem is not sufficiently ordered to ascertain whether it is correctly is positioned in the active site (*18*).

In the footprinting studies performed here, the appearance of protein-mediated increases in cleavage susceptibility for the mutant complex (Figures 4B, 5B, and 5C) were specifically localized to phosphates 5′ to nt 10, 23, 22, 47, and 50. These positions closely correspond to a subset of conserved tertiary interactions within the hinge region that stabilize the three-dimensional structure of the tRNA, reviewed in ref *48*. The importance of this region for tRNA binding in other class II aaRS systems is suggested both by the significant change in angle between the acceptor and anticodon arms of yeast $tRNA^{Asp}$ that is observed upon formation of the complex (*16*, *59*) and by the importance of tertiary determinants (*9*). An important caveat that must be noted regarding the footprinting data presented here is that these experiments provide only indirect evidence of potential interactions with the synthetase or of structural changes within the tRNA that correlate with changes in chemical reactivity of the probe. In any event, the footprinting results demonstrate that the mutant complex differs qualitatively from the wt complex. To critically evaluate whether changes in chemical reactivity are associated with conformational changes, additional mechanistic approaches will be necessary. In particular, the rate determining steps will have to be identified for wt and mutant complexes, so that the effects of specificity determining nucleotides can be correlated with the mechanism for aminoacylation.

ACKNOWLEDGMENT

The authors thank Laura Silvian for extensive discussions regarding filter binding. The generous assistance of Hans Beernink, Matthew Hockin, and Jed Pauls is acknowledged for the AUC studies. We thank Karin Musier-Forsyth for providing unpublished modifications to the iodine footprinting technique, and Anne-Catherine Dock-Bregeon for providing modified $tRNA^{Thr}$. Thanks also go to Karin Musier-Forsyth, Marie Sissler, John Arnez, Mark Rould, and Scott Morrical for critical reading of the manuscript.

REFERENCES

1. Park, S. J., and Schimmel, P. (1988) *J. Biol. Chem. 263*, 16527−30.
2. Arnez, J. G., and Moras, D. (1997) *Trends Biochem. Sci 22*, 211−6.
3. Eriani, G., Delarue, M., Poch, O., Gangloff, J., and Moras, D. (1990) *Nature 347*, 203−206.
4. Carter, C. W., Jr. (1993) *Annu. Rev. Biochem. 62*, 715−748.
5. Cusack, S. (1995) *Nature Struct. Biol. 2*, 824−831.
6. Francklyn, C., Musier-Forsyth, K., and Martinis, S. A. (1997) *RNA 3*, 954−960.
7. McClain, W. H. (1993) *J. Mol. Biol. 234*, 257−280.
8. Saks, M. E., Sampson, J. R., and Abelson, J. N. (1994) *Science 263*, 191−7.
9. Giegé, R., Sissler, M., and Florentz, C. (1998) *Nucl. Acids Res. 26*, 5017−5035.
10. Ebel, J. P., Giegé, R., Bonnet, J., Kern, D., Befort, N., Bollack, C., Fasiolo, F., Gangloff, J., and Dirheimer, G. (1973) *Biochimie 55*, 547−557.
11. Schimmel, P., and Söll, D. (1979) *Annu. Rev. Biochem. 48*, 601−648.
12. Perona, J. J., Swanson, R., Steitz, T. A., and Söll, D. (1988) *J. Mol. Biol. 202*, 121−126.
13. Rould, M. A., Perona, J. J., Söll, D., and Steitz, T. A. (1989) *Science 246*, 1135−1142.
14. Jahn, M., Rogers, M. J., and Söll, D. (1991) *Nature 352*, 258−260.
15. Pütz, J., Puglisi, J. D., Florentz, C., and Giegé, R. (1991) *Science 252*, 1696−9.
16. Ruff, M., Krishnaswamy, S., Boeglin, M., Poterszman, A., Mitschler, A., Podjarny, A., Rees, B., Thierry, J.-C., and Moras, D. (1991) *Science 252*, 1682−9.
17. Cavarelli, J., Eriani, G., Rees, B., Ruff, M., Boeglin, M., Mitschler, A., Martin, F., Gangloff, J., Thierry, J. C., and Moras, D. (1994) *EMBO J. 13*, 327−337.
18. Cusack, S., Yaremchuk, A., Krikliviy, I., and Tukalo, M. (1998) *Structure 6*, 101−8.
19. Cusack, S., Yaremchuk, A., and Tukalo, M. (1996) *EMBO J. 15*, 2834−2842.
20. Cusack, S., Yaremchuk, A., and Tukalo, M. (1996) *EMBO J. 15*, 6321−6334.
21. Ibba, M., Hong, K. W., Sherman, J. M., Sever, S., and Söll, D. (1996) *Proc. Natl. Acad. Sci. U.S.A. 93*, 6953−8.
22. Silvian, L. (1997) Ph.D. Thesis, Yale University, New Haven, CT.
23. Arnez, J. G., Harris, D. C., Mitschler, A., Rees, B., Francklyn, C. S., and Moras, D. (1995) *EMBO J. 14*, 4143−55.
24. Himeno, H., Hasegawa, T., Ueda, T., Watanabe, K., Miura, K., and Shimizu, M. (1989) *Nucl. Acids Res. 17*, 7855−7863.
25. Yan, W., and Francklyn, C. (1994) *J. Biol. Chem. 269*, 10022−10027.
26. Yan, W., Augustine, J., and Francklyn, C. (1996) *Biochemistry 35*, 6559−6568.
27. Francklyn, C., Harris, D., and Moras, D. (1994) *J. Mol. Biol. 241*, 275−277.
28. Francklyn, C., and Schimmel, P. (1990) *Proc. Natl. Acad. Sci. U.S.A. 87*, 8655−8659.
29. Yarus, M., and Berg, P. (1970) *Anal. Biochem. 35*, 450−465.
30. Wong, I., and Lohman, T. M. (1993) *Proc. Natl. Acad. Sci. U.S.A. 90*, 5428−5432.
31. Milligan, J. F., Groebe, D. R., Witherell, G. W., and Uhlenbeck, O. C. (1987) *Nucl. Acids Res. 15*, 8783−8798.
32. Lin, S.-Y., and Riggs, A. D. (1972) *J. Mol. Biol. 72*, 671−690.
33. Weeks, K. M., and Crothers, D. M. (1992) *Biochemistry 31*, 10281−10287.
34. Stafford, W. F. I. (1992) *Anal. Biochem. 203*, 295−301.

35. Laue, T. M., Shah, B. D., Ridgeway, T. M., and Pelletier, S. L. (1992) (Harding, S., and Rowe, A., Eds.) pp 90−125, Royal Society of Chemistry.
36. Cohen, G., and Eisenberg, H. (1968) *Biopolymers 6*, 1077−100.
37. Silberklang, M., Gillum, A. M., and RajBhandary, U. L. (1979) *Methods Enzymol. 59*, 58−109.
38. Augustine, J. G., and Francklyn, C. S. (1997) *Biochemistry 36*, 3473−3482.
39. Draper, D. E., Deckman, I. C., and Vartikar, J. V. (1988) *Methods Enzymol. 164*, 203−220.
40. Krauss, G., Römer, R., Reisner, D., and Maass, G. (1973) *FEBS Lett. 30*, 6−10.
41. Pingoud, A., Riesner, D., Boehme, D., and Maass, G. (1973) *FEBS Lett. 30*, 1−5.
42. Krauss, G., Pingoud, A., Boehme, D., Riesner, D., Peters, F., and Maass, G. (1975) *Eur. J. Biochem. 55*, 517−529.
43. Cavarelli, J., Rees, B., Thierry, J. C., and Moras, D. (1993) *Biochimie 75*, 1117−1123.
44. Schatz, D., Leberman, R., and Eckstein, F. (1991) *Proc. Natl. Acad. Sci. U.S.A. 88*, 6132−6.
45. Rudinger, J., Puglisi, J. D., Putz, J., Schatz, D., Eckstein, F., Florentz, C., and Giege, R. (1992) *Proc. Natl. Acad. Sci. U.S.A. 89*, 5882−6.
46. Nameki, N., Asahara, H., Shimizu, M., Okada, N., and Himeno, H. (1995) *Nucl. Acids Res. 23*, 389−394.
47. Sankaranarayanan, R., Dock-Bregeon, A.-C., Romby, P., Caillet, J., Springer, M., Rees, B., Ehresmann, C., Ehresmann, B., and Moras, D. (1999) *Cell 97*, 371−81.
48. Rich, A., and RajBhandary, U. L. (1976) *Annu. Rev. Biochem. 45*, 805−860.
49. Krauss, G., Riesner, D., and Maass, G. (1976) *Eur. J. Biochem. 68*, 81−93.
50. Krauss, G., Riesner, D., and Maass, G. (1977) *Nucl. Acids Res. 4*, 2253−62.
51. Arnez, J. G., Augustine, J. G., Moras, D., and Francklyn, C. S. (1997) *Proc. Natl. Acad. Sci. U.S.A. 94*, 7144−9.
52. Lam, S. S. M., and Schimmel, P. R. (1975) *Biochemistry 14*, 2775−2780.
53. Ebel, J. P., Giegé, R., Bonnet, J., Kern, D., Befort, N., Bollack, C., Fasiolo, F., Gangloff, J., and Dirheimer, G. (1973) *Biochem. Soc. Trans. 1*, 671−672.
54. Bonnet, J., and Ebel, J. P. (1975) *Eur. J. Biochem. 58*, 193−201.
55. Park, S. J., Hou, Y. M., and Schimmel, P. (1989) *Biochemistry 28*, 2740−6.
56. Sampson, J. R., and Uhlenbeck, O. C. (1988) *Proc. Natl. Acad. Sci. U.S.A. 85*, 1033−7.57.
57. Belrhali, H., Yaremchuk, A., Tukalo, M., Larsen, K., Berthet-Colominas, C., Leberman, R., Beijer, B., Sproat, B., Als-Nielsen, J., Grübel, G., Legrand, J.-F., Lehmann, M., and Cusack, S. (1994) *Science 263*, 1432−6.58.
58. Riesner, D., Pingoud, A., Boehme, D., Peters, F., and Maass, G. (1976) *Eur. J. Biochem. 68*, 71−80.59.
59. Westhof, E., Dumas, P., and Moras, D. (1985) *J. Mol. Biol. 184*, 119−145.

BI991182G